



How hard do we tap during snow stability tests?

Håvard B. Toft^{1,2}, Samuel V. Verplanck³ and Markus Landrø^{1,2}

¹The Norwegian Water Resources and Energy Directorate, Oslo, Norway

²Center for Avalanche Research and Education, UiT The Arctic University of Norway, Tromsø, Norway

5 ³Department of Mechanical Engineering, Montana State University, Bozeman, MT, 59717

Correspondence to: Håvard B. Toft, Norwegian Water Resources and Energy Directorate, Oslo, Norway; tel: +47 454 82 195; email: hsla@nve.no

Abstract. This study examines the impact force applied from hand taps during Extended Column Tests (ECT), a common method of assessing snow stability. The hand-tap loading method has inconsistencies across the United States, Canadian, and Norwegian written standards, as well as inherent subjectivity. We developed a device, the “tap-o-meter”, to measure the force-time curves during these taps and collected data from 286 practitioners, including avalanche forecasters and mountain guides in Scandinavia, Central Europe, and North America. Peak forces and loading rates are the metrics chosen to quantitatively compare the data. The mean, median, and inner quartile peak forces are distinctly different for each loading step (wrist, elbow and shoulder), as are the loading rates. However, there is significant overlap across the range of measurements and examples of participants with higher force wrist taps than other participants' shoulder taps. This overlap challenges the reliability and reproducibility of ECT results, potentially leading to dangerous interpretations in avalanche decision-making, forecasting and risk assessments. Therefore, we recommend updating the standards for the ECT. We propose two viable paths for future action: (1) define a target impact force-time curve for each tap level and develop tools and training to minimize variability in tapping force (2) assess the significance of the information derived from the number of taps. If deemed not highly valuable, we should consider reverting to a simpler binary interpretation that focuses exclusively on crack propagation.

1 Introduction

In the context of this discussion, snowpack stability describes the propensity of a snow-covered slope to avalanche (Reuter & Schweizer, 2011). It is inversely related to the probability of avalanche release and, therefore, a core concept in avalanche forecasting and backcountry decision-making. In backcountry travel, the decision process ultimately ends with a go or no-go decision based on an assessment of avalanche likelihood, avalanche size, and potential consequences. Snowpack stability evaluation is essential in assessing avalanche likelihood in such a context. In an avalanche forecasting setting, snow stability is divided into four classes: very poor (natural / very easy to trigger), poor (easy to trigger (e.g., a single skier), fair (difficult to trigger (e.g., explosives), and good (stable conditions). To determine the avalanche danger level for a region or forecast area at a point in time, forecasters in Europe use a matrix combining snowpack stability, snowpack stability frequency distribution, and avalanche size (Müller et al., 2023). Combined, snow stability and frequency are an expression of likelihood. The



frequency distribution of snowpack stability is described using four classes: many, some, a few, and none or nearly none. Using the European Avalanche Warning Service (EAWS) matrix, a combination of "very-easy-to-trigger," size 3-avalanches in "many" slopes leads to a danger level 4-high, whereas "difficult to trigger," size 3-avalanches in "many" slopes equals a danger level 3-considerable. This shows how an increase in stability effects the danger level, frequency being the same.

35

In situations with poor snowpack stability, nature provides apparent signs such as recent avalanches, shooting cracks, and "whumpfs". These signs are commonly referred to as Class I factors (instability factors) in a three-class division (LaChapelle, 1980; D. McClung & Schaerer, 2006). Unfortunately, the associated uncertainty increases for each class. The more stable the snowpack, the greater the load it can support before it fails. Instability can be less evident in these situations, and more indirect factors (class II -snowpack factors and class III meteorological factors) must be evaluated. Hence, stability tests (class II) can be of great importance in avalanche forecasting and provide highly valuable information to the backcountry traveler.

40

One of the first documented field snow tests is the shovel shear test developed by Faarlund and Kellermann in 1974 (originally known as the Norwegermethode; Kellermann, 1990). Although the role of compressive stress in weak layer failure was in discussion at the time (Perla & LaChapelle, 1970), weak layer shear strength - measured with a shear frame – was a typical metric for slope stability, and the shovel shear test provided a convenient field method of obtaining similar information.

45

In the late 1980s, Föhn (1987) quantified the Rutschblock (RB) test into the seven known levels today. In the 1990s, the compression test (CT) became popular (Clarkson, 1993; Jamieson & Johnston, 1996). The CT and RB involve loading the snow surface, transmitting stress through the slab, which may lead to weak layer failure.

50

The propensity for an initiated crack to propagate became a popular concept as a collapse-based, crack-propagation model (Heierli et al., 2008) had conflicting results with a shear-based, crack-propagation model (D. McClung, 1979). In line with this discussion, the propagation saw test (PST) (Gauthier & Jamieson, 2008, 2006) and extended column test (ECT) (Simenhois & Birkeland, 2006) were developed as field tests to assess propagation propensity.

55

Currently, the ECT is a frequently used test by avalanche practitioners and recreationists. The test has been validated in different avalanche climates such as continental and intercontinental climates of the United States (Birkeland & Simenhois, 2008; Hendrikx & Birkeland, 2008; Simenhois & Birkeland, 2009), the Swiss Alps (Techel et al., 2020; Winkler & Schweizer, 2009), the Spanish Pyrenees (Moner et al., 2008) and New Zealand (Hendrikx & Birkeland, 2008; Simenhois & Birkeland, 2006).

60

To conduct an ECT, a hand-tap loading method is implemented that was originally developed for the CT. There are subtle differences in the current guidelines for these taps. The most recent US standard, by American Avalanche Association (2022),
65 defines it as:

1. “Tap 10 times with fingertips, moving hand from wrist.”
2. “Tap 10 times with the fingertips or knuckles moving forearm from the elbow.”
3. “Hit the shovel blade moving the arm from the shoulder 10 times with open hand or fist”.

70 and the Canadian standard (Canadian Avalanche Association, 2016):

1. “Tap 10 times with fingertips, moving hand from wrist.”
2. “Tap 10 times with the fingertips or knuckles moving forearm from the elbow. While moderate taps should be harder than easy taps, they should not be as hard as one can reasonably tap with the knuckles”.
3. “Hit the shovel blade moving the arm from the shoulder 10 times with open hand or fist. If the moderate taps were
75 too hard, the operator will often try to hit the shovel with even more force for the hard taps - and may hurt his or her hand”.

And the Norwegian standard (Norwegian Water Resources and Energy Directorate, 2022).

“For every sequence of 10 taps, the load is increased as follows:

- 80
1. Let the hand fall with its own weight, lifted from the wrist.
 2. Let the hand and forearm fall with their own weight, lifted from the elbow.
 3. Let the entire arm fall with its own weight, using a fist, lifted from the shoulder.”

If a failure in the snowpack is detected during any of the taps, the specific tap number along with the depth of the weak layer
85 is recorded for further investigation. For example, if a failure propagates at the 21st tap at a depth of 40 cm, it would be noted as 'ECTP21@40cm. The interpretation of ECT test results remains an open discussion. Originally, a binary interpretation of test results was suggested, referred to as ECT_{orig} in this paper. Specifically, if a fracture initiates but does not propagate (ECTN), then the test result is considered stable. In contrast, if a fracture propagates across the extended column (ECTP, or ECTPV if during isolation), then the test result is considered unstable. The test result is ECT_{EX} if no fracture occurs.

90

Another classification was suggested by Winkler and Schweizer in 2009 (ECT_{w09}), using three classes divided by the number of taps needed to initiate a fracture with or without propagation:

- $ECTP \leq 21$ – low stability
- $ECTP > 21$ – intermediate stability
- ECTN or ECTX – high stability

95



Recent work by Techel et al. (2020) (ECT_{120}) suggests using four classes and applying the established labels for snow stability: poor, fair and good (i.e. American Avalanche Association, 2022):

- $ECTP \leq 13$ – poor
- 100 • $ECTP > 13$ to $ECTP \leq 22$ – poor to fair
- $ECTP > 22$ or $ECTN \leq 10$ – fair
- $ECTN > 10$ or $ECTX$ – good

The variability in tapping force has been a known limitation for the CT and ECT interpretation (American Avalanche
105 Association, 2022; Schweizer & Jamieson, 2010; Techel et al., 2020). Birkeland and Johnson (1999) attempted to remedy this limitation by developing the stuffblock test. The test uses a nylon sack filled with ~4.5 kg (10 pounds) of snow which is dropped on a CT or ECT column with 10 cm increments until a result is reached.

There have been some previous studies to measure the applied force of hand tapping, as well as quantify the stress-state within
110 the snow during these loads. Logan (2006) made measurements of hand taps during a conference to learn more about timing, impact force and technique, but the results were never published. Thumlert and Jamieson (2015) impacted the snow with both a drop hammer and hand taps and measured the resulting stress within the snow. Griesser et al. (2023) measured the impact force from 62 participants from the European Avalanche Warning Services, as well as a field-based study where they measured stress within the snowpack.

The objective of our work is to characterize the impact curves of the hand-tap loading and investigate the variability between
120 participants. Determining how this applied force interacts with snow is outside of our scope, however, a quantified understanding of how practitioners are loading the snow would aid in test result interpretation. In addition, this study will aid in the mathematical modeling of stability tests.

By modeling stability tests, researchers can gain insight into the avalanche release process and quantify key parameters such
as the effective elastic modulus of the slab and weak layer fracture energy (van Herwijnen et al., 2016). Modeling efforts have focused on the PST rather than the CT or ECT (Benedetti et al., 2019; McClung & Borstad, 2012; Weißgraeber & Rosendahl, 2023). One reason is the crack is initiated by cutting through the weak layer with a snow saw during the PST, a more measurable
125 mechanism than the impact-initiated crack of the CT/ECT. Although our study does not attempt to model the CT/ECT, characterizing the force-time curves of hand taps is a step towards a more scientific understanding of these tests.



2 Methods

2.1 The device: tap-o-meter

130 To measure the force from hand taps, a device dubbed the tap-o-meter was made. A total of three devices were built to enable data collection in different parts of the world in a similar time frame (Fig. 1). Each tap-o-meter has the following components:

1. A shovel blade which acts as the loaded surface.
2. A load cell to transduce the tapping force into an electric signal.
3. Oscilloscope with a voltage amplifier to measure the signal.
4. 30 x 30 x 0.6 cm stainless steel base to provide a sturdy foundation.

135 2.1.1 Load cell

A single, cantilever-style load cell from Load Cell Central (GCB3-SS-M-50KG) was used to measure the tapping force. The recommended capacity of the load cell is 490 N, with an ultimate overload rating of 1,470 N. The full-scale output (FSO) of the load cell is 2 mV/V and refers to the maximum output signal that the load cell can produce for its rated capacity.

2.1.2 Oscilloscope and voltage amplifier

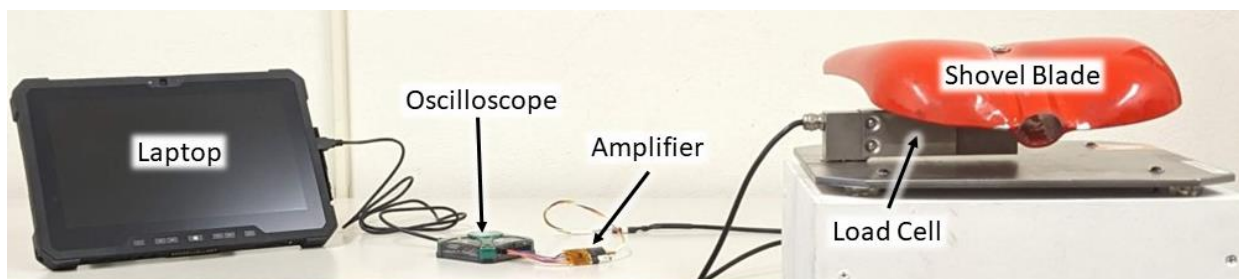
140 An oscilloscope (Digilent Analog Discovery II) was used to measure the impact force. The oscilloscope provides a 5-volt input to the load cell, which yields a maximum output signal of 10 mV with the FSO from the load cell. The minimum change in voltage that can be measured by the oscilloscope is 0.2 mV. To increase the measurement resolution, a voltage amplifier was added between the load cell and the oscilloscope. The amplifier was custom built using an AD8429 amplifier from Analog Devices. The amplification, or gain (G), is controlled by an external two-pin resistor (R_{ext}), using the following equation:

145

$$G = 1 + \frac{6000 \text{ ohm}}{R_{ext}}, \quad (1)$$

In our study, we used a 30-ohm resistor, resulting in a 201x amplification of the output signal from the load cell. Using this setup, the oscilloscope is theoretically able to measure 10,050 steps between 0-490 Newtons, or 30,150 loading steps between 0-1,470 N. The device was calibrated statically by using a set of known masses ranging from ~5 to 30 kg (Appendix-1) and a linear regression ($R^2 = 0.999998$).

150



155 **Figure 1: The tap-o-meter consists of a metal base with the load cell and shovel blade attached above. The load cell is connected to the oscilloscope through the custom-built 201x amplifier.**

To determine an appropriate sampling rate, knowledge of the impact signal is critical. We are most interested in the peak force and loading rate leading up to it. Preliminary testing showed that this rise time is fastest for the shoulder taps and can happen as quickly as a few milliseconds. Conservatively assuming this rise occurs over 1 millisecond, a sampling rate of 50 kHz leads to 50 samples in this critical measurement period. A number deemed sufficient for our purposes and within the capabilities of the measurement system.


2.2 Data collection process

Data collection was conducted at events in Norway, Switzerland, Austria, USA and Canada. In Norway, data was collected from avalanche forecasters and mountain guides. In Switzerland, data was collected at the EAWS general assembly. Canadian and Austrian events only included avalanche forecasters. Events in the US contained a mix of avalanche workshop participants and avalanche forecasters.

We made the setup as similar as possible by using three identical tap-o-meter devices. All tap-o-meters were firmly attached to a wooden CT (30 x 30 x 85 cm) or ECT (30 x 90 x 85 cm) column (Fig. 1). By using a fixed height, we acquired data with a consistent sampling method but are not able to adjust for changes in snowpack thickness. Furthermore, participants were given the choice to use different types of gloves depending on their preferences. The intent was that all participants should be able to conduct the test like they would do in the field. However, we left the shovel handle off. We did this because the user may grab the shovel handle and touch the load cell, leading to an inaccurate measurement.

2.2.1 Survey

175 For each participant, we asked them to fill out a survey where they noted their country of residency, avalanche climate, height, weight and gender. The information from the survey was collected to answer the following research questions:

1. Does height, weight, and/or gender affect tapping force?
2. Do people tap differently across avalanche climates?
3. Are there regional differences between Scandinavia, Alps and North America? 

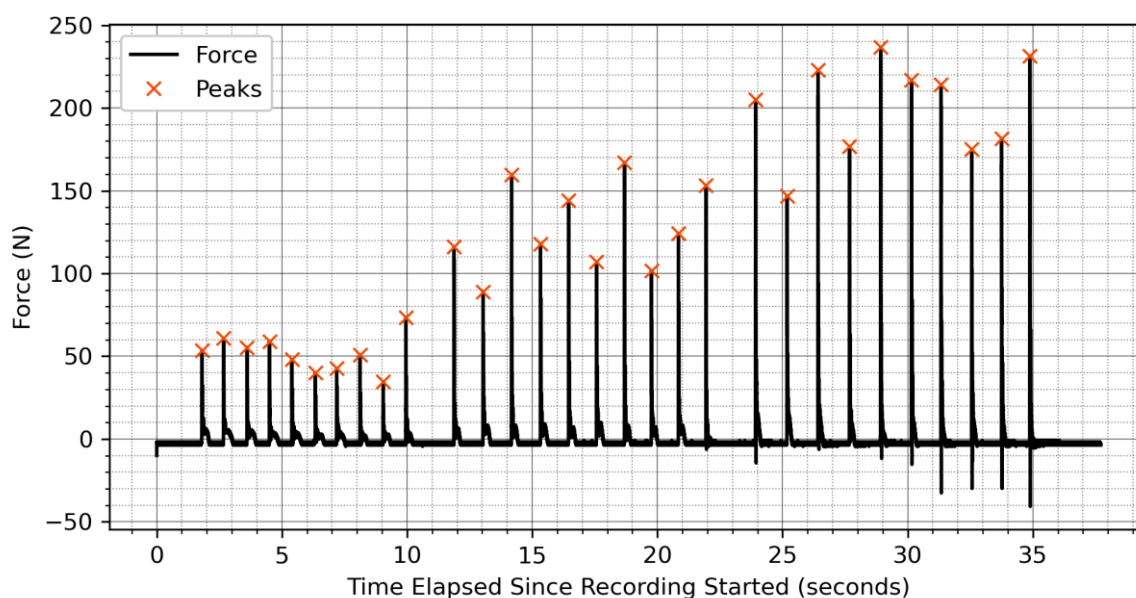


180 2.3 Data processing

The raw voltage data are processed using python to identify the individual taps. After the taps are identified, two metrics are pulled from each one: maximum force (newtons, N) and loading rate (N/s).

185 The recorded time and voltage are imported as NumPy arrays (Harris et al., 2020). The voltage values are zeroed by subtracting the array's mean from each data point. Then, voltage is converted to newtons by scaling according to the calibration. Scipy's (Virtanen et al., 2020) peak finding algorithm is implemented to determine when the taps occur. The peak finding algorithm is driven with two parameters: a 25 N minimum peak magnitude and 0.4 seconds minimum time between peaks. These criteria are chosen by iteratively trying different values and viewing the results. This peak finding method is used as a first pass through the data and is later refined with a more manual process. See Figure 2 for an example of tap data with the peaks algorithmically identified.
190 identified.

Recorded Time Series of Force with Identified Peaks



195 **Figure 2: The result of identifying taps using SciPy's peak finding algorithm with 25 N minimum peak magnitude and a minimum of 0.4 seconds between peaks. Using these parameters, the algorithm correctly identified all peaks as it did in 262/286 cases. Manual adjustments to the algorithm's parameters were used in the remaining 24 cases to identify peaks.**

After the peaks are found the individual taps are defined as 70 ms prior to and 40 ms after the peak. These values are chosen to allow for enough time surrounding the peak to determine tap metrics. Each tap array is then re-zeroed by subtracting the mean of the first 0.2 ms of that specific tap. This re-zeroing process is implemented because subtle shifts in the baseline recording are occasionally apparent, particularly during the taps hinging from the wrist if the tapper kept contact with the



200 shovel blade throughout these taps. The two metrics, maximum force and loading rate, are ascertained from each tap array. Maximum force is simply the maximum value in the re-zeroed array. The loading rate is defined as a linear interpolation, Eq. (2), between the maximum force and when the force curve crosses a 15 N threshold, signifying the start of impact. A threshold chosen because it is greater than typical noise. The difference in force is divided by the rise time to determine the loading rate. The rise time is the difference in time between the peak force and the start of the ta

205
$$\text{Loading rate} = \frac{\text{Max force}}{\text{Rise Time}}, \quad (2)$$

After this automated process is applied to all 286 tap recordings, a manual quality control process is done. This process entails viewing the taps for each recording (Fig. 3), flagging misidentified taps, and classifying which taps are hinging from the wrist, elbow and shoulder. This manual process determined that 262/286 recordings were correctly processed with the first-pass algorithm. The remaining 24 recordings were reprocessed by changing the parameters for SciPy’s peak finding algorithm. The changes to peak-finding parameters involved reducing the time between peaks or minimum magnitude until all the clear taps are identified. In some cases, the metrics were not calculated accurately because there was a spike of noise that was close enough in time to the tap signal. In these cases, the individual taps were not included in the analyzed data set. After this second processing step, the data set is ready for analysis.

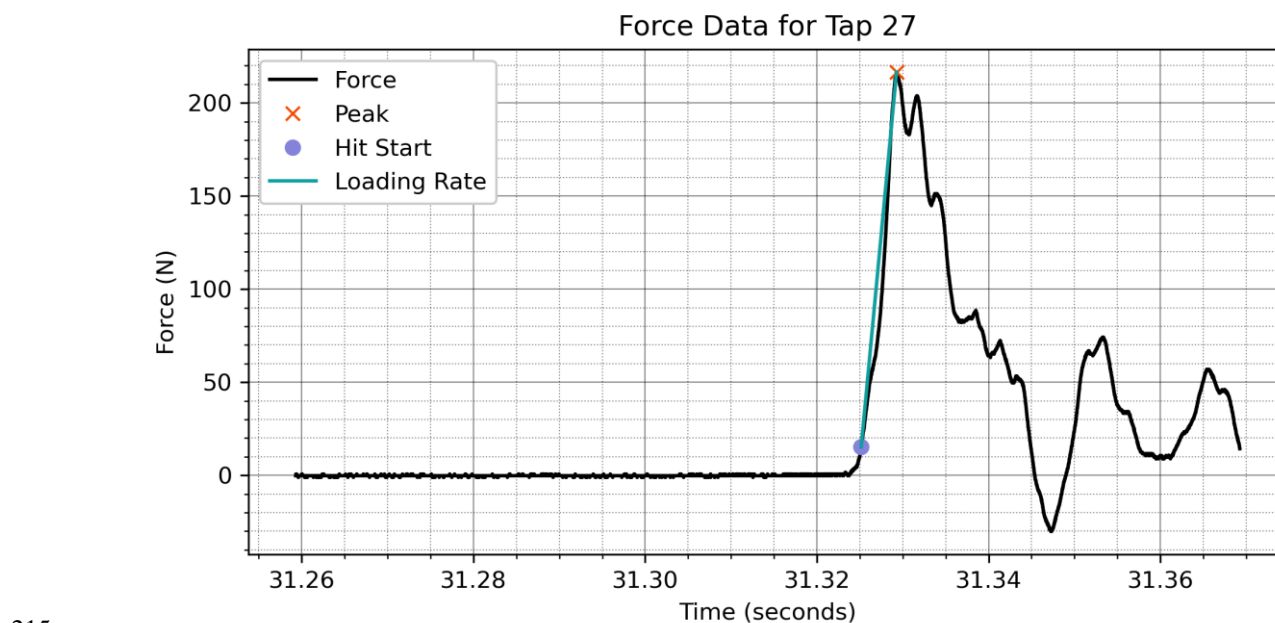


Figure 3: An example of the data processing procedure implemented on a shoulder tap. This procedure acquires two metrics for each tap: peak force (N) and loading rate (N/s).



3. Results

220 The data set consists of 2,837 wrist taps, 2,839 elbow taps, and 2,846 shoulder taps across 286 individuals. Outliers are excluded using 1.5 times the interquartile range (IQR) method, which is a widely recognized and accepted standard in statistical analysis (Tukey, 1977). For peak force, we excluded 132 taps for wrist, 106 taps for elbow and 120 taps for shoulder as outliers. Saturation occurred in rare instances due to a limitation with the amplifier in the tap-o-meter: it happened once during elbow taps and 75 times during shoulder-level taps (Table 1). More on this in section 4.1.1.

225

Table 1: Number of taps, outliers and saturation taps for peak force and loading rate.

	Peak Force			Loading Rate		
	Wrist	Elbow	Shoulder	Wrist	Elbow	Shoulder
No. of taps	2,837	2,839	2,846	2,837	2,839	2,846
No. of outlier taps	132	106	120	145	116	204
No. of saturation taps	0	1	75	0	0	0

For peak force, the average wrist tap force recorded is 85 N with a standard deviation of 47 N. At elbow taps, the average force is higher at 196 N, with a standard deviation of 104 N. The shoulder taps are the powerful having an average peak force of 400 N, with a standard deviation of 211 N. The maximum peak force for the wrist, elbow, and shoulder levels are 190 N, 426 N, and 893 N respectively (Table 2).

230

The loading rates are presented for the same three tap levels. The wrist taps, have an average loading rate of 11,263 N/s with a standard deviation of 34,563 N/s. The elbow taps, show an average loading rate of 31,752 N/s with a standard deviation of 23,179 N/s. The shoulder level has the highest average loading rates at 86,179 N/s with a standard deviation of 79,202 N/s. The maximal loading rates for the wrist, elbow, and shoulder levels are 30,145 N/s, 81,619 N/s, and 195,811 N/s respectively (Table 2).

235

Table 2: Descriptive statistics of peak force and loading rate (outliers removed using 1.5 * IQR).

	Peak Force (N)			Loading Rate (N/s)		
	Wrist	Elbow	Shoulder	Wrist	Elbow	Shoulder
Mean	85	196	400	11,263	31,752	86,179
Std.	47	104	211	34,563	23,179	79,202
Min	8	34	45	118	149	2,316
25 th percentile	51	125	244	3,572	15,550	38,771
Median	74	175	352	7,379	25,982	65,560

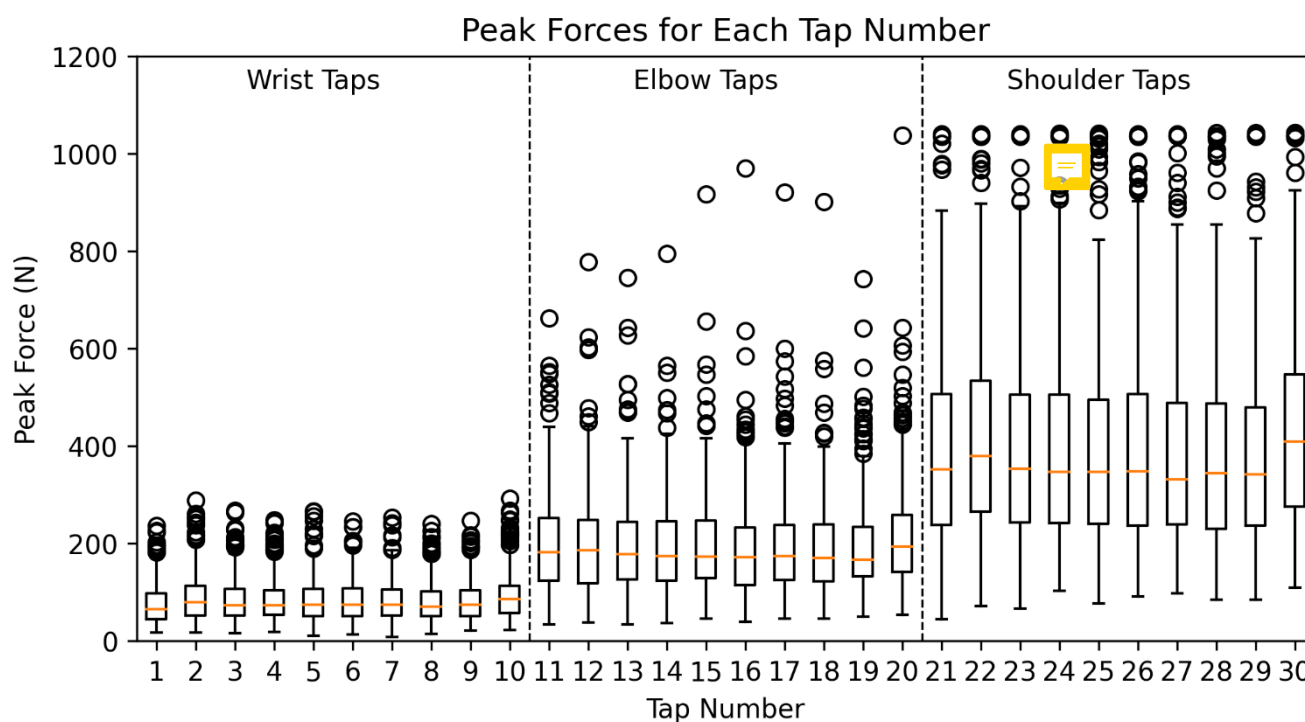


75 th percentile	107	245	505	14,238	42,016	101,673
Max	190	426	893	30,145	81,619	195,811

240

3.1 Trends and variability by individual tappers

In Figure 4, the distribution of peak forces across different tap numbers is graphically represented for three tapping levels: wrist, elbow, and shoulder. For each tap number, a boxplot illustrates the interquartile range, with the median force denoted by an orange horizontal line. Individual outliers, shown as circles, showcase the spread of peak forces. While the median forces across each tap level remain relatively consistent, there is a large spread across all tap levels. Collectively, this figure emphasizes the inherent differences in peak forces across the three tapping levels and underscores the variability present within each level across different tap numbers.



250 Figure 4: A visualization of the magnitude and variability in peak impact force from the 286 participants from tap 1 to 30. A box plot for each tap number displays the minimum, first quartile, median, third quartile, and maximum values. Outliers are shown using circular symbols. The load cell reaches saturation at 1,000 N, a threshold which was reached in one elbow tap and 75 shoulder taps.



3.2 Survey results

255 In our effort to understand the underlying factors influencing tapping force, we performed a set of multivariate regression models (Ordinary Least Squares). More specifically, we tested if height, weight, gender, geographic region, and avalanche climate affected the impact force during tests. Due to the small sample size from various snow climates, it was impossible to include this factor in the multivariate regression models. To avoid collinearity issues, we evaluated the role of snow climate in a separate, single-variable regression.

260

There are two important findings from the regression models. First, the information contained in the explanatory variables cannot explain the bulk of the variance in the tap-o-meter data. Second, weight and height are significantly and positively correlated with tap force as individual explanatory variables; however, the significance is no longer apparent when we include gender. Thus, gender is the only explanatory variable that is significantly correlated with tap force across all multivariate

265

regression models.

Due to the poor fit of the models and the small sample size, we only present results from simple bivariate tests (Student t-tests) here. For wrist taps, men on average tap at 88 N while women's average is at 71 N ($t = 2.83$, $p < 0.001$). For elbow taps, men on average tap at 205 N while women's average is at 160 N ($t = 3.53$, $p < 0.001$). For shoulder taps, men on average tap at 420 N while women's average is at 316 N ($t = 4.12$, $p < 0.01$).

270

3.3 Idealization of taps as Gaussian functions

Both the peak force and loading rate are used to idealize the impact curves. First, consider the equation describing a Gaussian function.

$$F(t) = F_{peak} e^{-\frac{1}{2} \left(\frac{t-t_{peak}}{s} \right)^2}, \quad (3)$$

275 Where F_{peak} is the peak force and t_{peak} is the time at which the peak force occurs. The duration of the force curve is governed by s , the standard deviation if the Gaussian function were to be describing a normal distribution. Since 99.7% of the curve's magnitude occurs during $6s$, the duration of impact is defined $6s$ in our study. Thus, the rise to peak force occurs over approximately $3s$.

$$loading\ rate \approx \frac{F_{peak}}{3s}, \quad (4)$$

280 This is an approximation rather than equality because it assumes a linear rise, rather than the non-linear Gaussian shape. However, since loading rate and peak force are the two metrics ascertained from the measured data, this approximation provides a convenient way to idealize the measured force curves. Rearranging the approximation yields

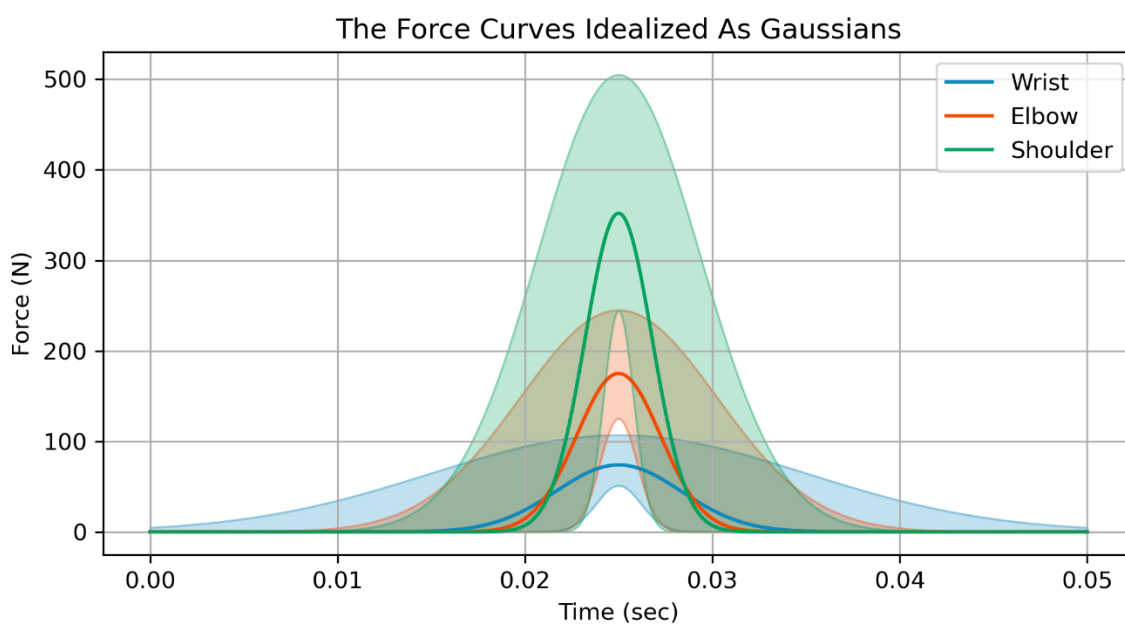


$$s \approx \frac{F_{peak}}{3 * (loading\ rate)}, \quad (5)$$

285 And substituting this relationship for s in Eq. (3) yields the Gaussian approximation used to idealize the measured force-time curves.

$$F(t) \approx F_{peak} e^{-\frac{1}{2} \left(\frac{3 * (t - t_{peak}) * (loading\ rate)}{F_{peak}} \right)^2}, \quad (6)$$

Using the median metrics along with their 25th and 75th percentiles are plotted in Figure 5.



290 **Figure 5: An idealization of the taps as Gaussian functions. The center lines are from the median metrics and the shading is generated from the 25th and 75th percentiles.**

By idealizing these tap curves as Gaussians, their respective impulses (i.e. momentums) can be compared by calculating the area under curve. Using NumPy's implementation of the trapezoidal rule (Harris et al., 2020), the median wrist, elbow, and shoulder tap impulses are 0.62, 0.99, and 1.58 N*s, respectively.



295 4. Discussion

4.1 Methods

4.1.1 The tap-o-meter

The tap-o-meter was initially developed using parts in stock at the Norwegian Water Resources and Energy Directorate (NVE). Early testing suggested that a 50 kg load cell which NVE had in stock would be capable of accurately recording the impact force from taps. Based on data collected prior to those showcased in this paper, it became evident that the impact forces from some participants plateaued around 600 N (~60 kg) on their shoulder taps. This level surpassed the recommended operating range of the load cell but stayed within the ultimate overload capacity (150 kg). We pinpointed the problem to the amplifier, which was reaching its saturation point.

We considered the amplifier properties to avoid two potential issues. Setting it too high would mean losing detail in measuring light wrist taps due an increased background noise. On the other hand, setting it too low would make it impossible to measure the strongest impact forces.

To address this, we developed a new adjustable amplifier that we tuned to a range from 5 to 1,000 N. This calibration aimed to balance the ability to detect high-impact forces while maintaining a low background noise for measuring the force of lighter taps. The defined range stayed safely below the load cell's ultimate overload threshold of 1,225 N. Despite the new adjustment with the amplifier's upper limit set to 1,000 N, saturation still occurred in rare instances: once during elbow-level taps (representing 0.03% of such taps) and 75 times for shoulder-level taps (2.63% of such taps). All of these taps are identified as outliers (Figure 4).

The tap-o-meter was calibrated by stacking steel plates of known mass on the load cell. The calibrated range was limited to 30 kg (294 N) to prevent the masses from tipping over and maintain even load distribution. In our analyses, we are assuming the load cell continues to respond linearly through its working range up to its operating limit. Thus, the upper end of shoulder tap measurements may not be accurate. Furthermore, we are assuming the load cell responds similarly to dynamic load as static loads and eccentric loads as centered loads. These potential inaccuracies in the measurement technique, likely contribute to the range and variability of force measured in this study. Future studies should include a load cell with a higher range (e.g. 200 kg), load cells designed for impacts (e.g. piezo-resistive), and a fixture to ensure centered loading. Despite these potential measurement inaccuracies, our study utilized a sampling rate (50 kHz) appropriate for capturing the entirety of the impact curve. This is an improvement over similar studies that used a sampling rate of 100 Hz. (Griesser et al. 2023) and 105 Hz (Thumlert and Jamieson, 2015).



325 **4.1.2 Data collection**

Initially, our idea was to have a representative group of participants with different levels of training. However, after the first data collection event, we realized that most novices did not know how to do the test, and it was difficult to get a representative sample from less experienced participants.

330 Each participant was asked to fill out a survey. In retrospect, an estimate of how many ECTs each participant does in a season would be of interest. Most participants noted that they do it regularly at work, recreation or both, but we do not have an idea of how frequently they conduct ECTs.

Furthermore, systematic notes about the tapping technique would also be of interest. A qualitative remark is that many of the participants do not use their fingertips on wrist taps as in the standards (American Avalanche Association, 2022; Canadian
335 Avalanche Association, 2016). There was also a large variability in impact forces as a result of using the weight of the arm versus a shoulder tap so hard that it hurts the hand. In some cases, participants placed a glove on the shove to soften the blow. We also observed that some participants increased their impact force during the ten taps within each level, but we do not see this in our overall data (Fig. 4).

340 **4.1.3 Metric Selection**

To gain a quantitative understanding of the collected data, peak force and loading rate were the chosen metrics. Other quantities such as impact duration, rise time, and stress were considered but not chosen. Impact duration was not used because the measurements frequently contained long, oscillatory tails that are an artifact of the load cell rebounding and vibrating – a phenomenon expected to be less present during an actual field test. Rise time was calculated as an intermediary step to loading
345 rate. However, loading rate was chosen because snow's response has been shown to depend on its rate of deformation (Shapiro et al., 1997). Lastly, our measurements are presented as forces (N) rather than stresses (kPa) because presenting it as a stress would rely on an assumption of cross-sectional area.

4.2. Results

Using the data from the tap-o-meter, we are able to provide insight into the impact forces of hand taps and the variability
350 between participants. We believe the quantification of the magnitudes and variabilities associated with hand-tap loading will assist with our understanding and interpretation of the ECT and CT.

4.2.1 Impact force

When interpreting the descriptive definitions from each tap level, it is impossible to infer which impact forces should be used as a baseline for each tap level. For example, the Norwegian description (Norwegian Water Resources and Energy Directorate,



355 2022) using the arm's weight would depend on the weight of each participant's arm. Furthermore, in Canada, there is no
description of how hard each tap should be other than that it should not hurt at shoulder level (Canadian Avalanche Association,
2016). However, this would depend on the participant's pain tolerance, snow properties (dampening) and the participant's glove
thickness. The impact forces presented in this paper could be used as a baseline for future clarifications if a “wisdom of crowds”
impact force definition is employed (see Surowiecki, 2005 for an introduction to the concept of "wisdom of crowds”).
360 Furthermore, a training device could be developed that measures the impact force and reports back to the participants whether
they are within the correct window at each tap level. Such devices already exist for CPR training and provides real-time
measured feedback on compression rate (cpm), depth (mm), release (g), compressions count, and inactivity time during CPR,
while also enabling responders to self-evaluate their performance with event statistics on the spot (Laerdal, 2023).

4.2.2 Variability between participants

365 In our study involving 286 participants, we observe different mean and median values for each tap level. If we consider the
interquartile range which represents the data between the 25th and 75th percentile, there is nearly no overlap between tap levels.
However, when considering the range of data (excluding outliers), from the minimum to the maximum values (as represented
by the whiskers in a Fig. 4), there is a considerable degree of overlap. This suggests that fifty percent of the data is distinctly
different for each tap level. On the other hand, that implies that up to fifty percent of the data could overlap with other tap
370 levels. Furthermore, there are examples of participants with harder wrist taps than other participants' shoulder taps. This has
implications for the consistency and reliability of the test results.

4.2.3 Idealization of taps as Gaussian functions

The Gaussian function is often used in wave propagation problems because it represents a smooth, continuous pulse of
disturbance (Langtangen & Linge, 2017). The measured shape of force-time curves is not a perfect Gaussian (Fig. 3),
375 particularly after the peak force has been reached. The noisy, oscillatory decay following the peak is attributed, in part, to the
instrumentation. Despite these imperfections, we intend to show this idealization as a steppingstone towards mathematical
modelling efforts.

4.3 Future work

During data collection, we asked participants if they regularly conduct CTs or ECTs for work, recreation or both. Participants
380 were also asked to self-evaluate their avalanche assessment level on a scale from 1 to 6, following the definitions from the
CARE-panel study (Hetland & Mannberg, 2023). Our hypothesis was that more experienced participants, particularly those
frequently performing stability tests, would be more consistent within each loading step. However, the study's shift in focus
towards more experienced individuals (see Section 4.1.2) meant that we lacked a suitable reference group for comparison. For
future studies, a more effective approach might involve quantifying the frequency of CTs or ECTs performed by each



385 participant per season. This method could provide a more nuanced understanding of the relationship between the quantitative
experience and tapping consistency.

Snow's response to impact forces remains an active research topic and is out of the scope of this study. However, variability
in magnitude and duration of applied force will result in some variability of the stress state within the snow which may lead to
390 variability in test results. For more on this topic, we refer the reader to studies by Napadensky (1964), Wakahama & Sato
(1977), Johnson et al. (1993), Schweizer et al. (1995), van Herwijnen & Birkeland (2014), Thumlert & Jamieson (2015), and
Griesser et al. (2023).

5. Conclusion

The main finding from our study is that there is a substantial variability in impact force among individuals conducting ECTs.
395 The inconsistency challenges the reliability and reproducibility of ECT results, potentially leading to dangerous interpretations
in avalanche decision-making, forecasting and risk assessments. Therefore, we recommend updating the standard for the ECT.
How the standard should be updated, specifically, should be a decision made collaboratively by the broader avalanche
community.

5.1 Calls to action

400 Given the variability in tapping demonstrated in this study, we propose two paths to improve the ECT standards. The two paths
outlined below are intended to be a foundation for further discussion in the broader avalanche community.

5.1.1 Reduce tapping variability through the use of training and/or tools.

The large variability in impact force between individual participants highlights the need for standardization. This could be
done by creating a better definition of how the test should be conducted in terms of tapping force and technique. The community
405 will need to agree on what the ideal impact force-time curves are. A “wisdom of crowds” approach could be taken and the
median values in our study could be used, or a selection of experts could choose to define these windows. With these windows
defined, a training device could be developed that measures the impact force and reports back to the participants whether they
are within the correct window at each hand tap level. Another solution could be to develop a tool that ensures consistent impact
force (e.g., stuffblock test or known weights).

410 5.1.2 Limit the test's interpretation

Another path would be to limit the level of detail in test result interpretation. As members of the international avalanche
community, we need to assess whether the number of taps holds significant value in interpreting ECT results. The added
complexity from Winkler et al. (2009) and Techel et al. (2020) makes the test more dependent on the individual's impact force.



If we do not deem the number of taps to be important, we could revert to the original, binary interpretation from Simenhois
415 and Birkeland (2006), focusing solely on crack propagation. In this approach, we would consider the test result to be unstable
if crack propagation occurs, and stable otherwise. This interpretation merits the question of why having three steps in the
loading procedure. If the community aims to maintain consistency in this three-step loading method, it should adopt a refined
version of the standards currently used in the United States, Canada, and Norway.

Data availability

420 The data needed to replicate the study is available in our Open Science Framework repository (Toft et al., 2023).

Author contributions

The study was conceptualized by HT, SV, and ML. HT developed and built the three tap-o-meters. All authors actively
participated in data collection at various events. SV, with HT's assistance, conducted the data pre-processing. HT led the
analysis on trends and variability among participants, incorporating insights from SV and ML. The conceptualization of taps
425 as Gaussian functions was primarily driven by SV, with inputs from HT and ML. All authors were actively involved in the
preparation, editing, and review of the original draft.

Acknowledgements

We would like to acknowledge Knut Møen for his technical contributions to the development of the tap-o-meter and for his
creative input in naming the device. Furthermore, Andrea Mannberg for her statistical expertise, Christoph Mitterer and Scott
430 Savage for assistance in data collection – with additional thanks to Scott for facilitating us while working on this in Idaho.
Jordy Hendriks for connecting the authors, a collaboration born out of the realization that we were doing similar work. Thank
you to all of the study participants as well.

Competing interests

The authors declare that they have no conflict of interest.

References

American Avalanche Association. (2022). Snow, Weather and Avalanches: Observation Guidelines for Avalanche Programs
in the United States. In E. Greene, K. Birkeland, K. Elder, I. McCammon, M. Staples, D. Sharaf, S. Trautman, & W.
Wagner (Eds.), *American Avalanche Association* (4th Edition). American Avalanche Association.



- Benedetti, L., Gaume, J., & Fischer, J.-T. (2019). A mechanically-based model of snow slab and weak layer fracture in the
440 Propagation Saw Test. *International Journal of Solids and Structures*, 158, 1–20.
<https://doi.org/10.1016/j.ijsolstr.2017.12.033>
- Birkeland, K. W., & Johnson, R. F. (1999). The stuffblock snow stability test: comparability with the rutschblock, usefulness
in different snow climates, and repeatability between observers. *Cold Regions Science and Technology*, 30(1–3), 115–
123. [https://doi.org/10.1016/S0165-232X\(99\)00015-4](https://doi.org/10.1016/S0165-232X(99)00015-4)
- 445 Birkeland, K. W., & Simenhois, R. (2008). The Extended Column Test: Test Effectiveness, Spatial Variability, and
Comparison with the Propagation Saw Test. *International Snow Science Workshop, Whistler, British Columbia*, 867–
874.
- Canadian Avalanche Association. (2016). Observation guidelines and recording standards for weather, snowpack and
avalanches. In C. Campbell, D. McClung, B. Jamieson, B. Sayer, R. Whelan, J. Floyer, & S. Garvin (Eds.), *Canadian*
450 *Avalanche Association* (6th Edition). Canadian Avalanche Association.
- Clarkson, P. (1993). Compression test. *Avalanche News* 40, 9–9.
- Föhn, P. (1987). The rutschblock as a practical tool for slope stability evaluation. *IAHS Publ*, 162, 223–228.
- Gauthier, D., & Jamieson, B. (2008). Fracture propagation propensity in relation to snow slab avalanche release: Validating
the Propagation Saw Test. *Geophysical Research Letters*, 35(13), 2–5. <https://doi.org/10.1029/2008GL034245>
- 455 Gauthier, D., & Jamieson, J. B. (2006). Evaluating a prototype field test for weak layer fracture and failure propagation.
International Snow Science Workshop, Telluride, Colorado, 107–116.
- Griesser, S., Pielmeier, C., Boutera Toft, H., & Reiweger, I. (2023). Stress measurements in the weak layer during snow
stability tests. *Annals of Glaciology*, 1–7. <https://doi.org/10.1017/aog.2023.49>
- Harris, C. R., Millman, K. J., van der Walt, S. J., Gommers, R., Virtanen, P., Cournapeau, D., Wieser, E., Taylor, J., Berg, S.,
460 Smith, N. J., Kern, R., Picus, M., Hoyer, S., van Kerkwijk, M. H., Brett, M., Haldane, A., del Río, J. F., Wiebe, M.,
Peterson, P., ... Oliphant, T. E. (2020). Array programming with NumPy. *Nature*, 585(7825), 357–362.
<https://doi.org/10.1038/s41586-020-2649-2>
- Heierli, J., Gumbsch, P., & Zaiser, M. (2008). Anticrack nucleation as triggering mechanism for snow slab avalanches. *Science*,
321(5886), 240–243. <https://doi.org/10.1126/science.1153948>
- 465 Hendrikx, J., & Birkeland, K. (2008). Slope Scale Spatial Variability Across Time and Space: Comparison of Results from
Two Different Snow Climates. *International Snow Science Workshop, Whistler, British Columbia*, 155–162.
- Hetland, A., & Mannberg, A. (2023). CARE Panel. UiT The Arctic University of Norway. <https://uit.no/research/carepanel>
- Jamieson, B., & Johnston, C. (1996). The Compression Test for Snow Stability. *International Snow Science Workshop, Banff,*
Alberta, 118–125.
- 470 Johnson, J. B., Solie, D. J., Brown, Joseph. A., & Gaffney, E. S. (1993). Shock response of snow. *Journal of Applied Physics*,
73(10), 4852–4861. <https://doi.org/10.1063/1.353801>



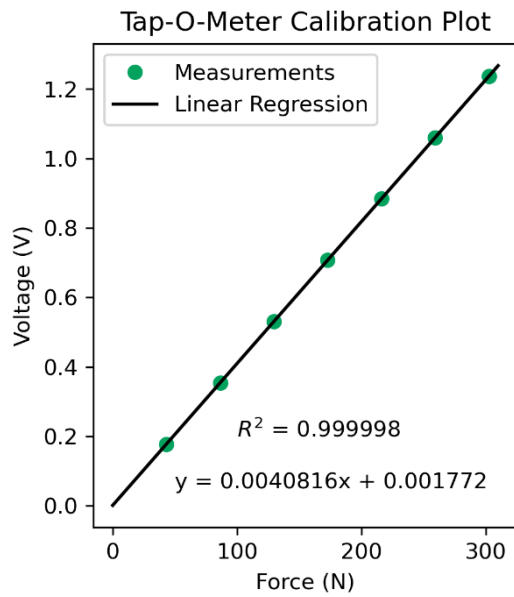
- Kellermann, W. (1990). Erfahrungen mit der Norwegermethode und deren Vergleich mit dem Rutschblock/Keil. In W. Kellermann (Ed.), *Vortrag beim Zentralen Kaderkurs Lawinen des SAC*. Swiss Alpine Club.
- LaChapelle, E. R. (1980). The Fundamental Processes in Conventional Alavalanche Forecasting. *Journal of Glaciology*, 26(94), 75–84. <https://doi.org/10.3189/S0022143000010601>
- Laerdal. (2023). *CPRmeter 2 User Guide*. Laerdal. https://cdn.laerdal.com/downloads/f6537/cprmeter_2_user_guide_en
- Langtangen, H. P., & Linge, S. (2017). *Finite Difference Computing with PDEs* (Vol. 16). Springer International Publishing. <https://doi.org/10.1007/978-3-319-55456-3>
- McClung, D. (1979). Shear fracture precipitated by strain softening as a mechanism of dry slab avalanche release. *Journal of Geophysical Research: Solid Earth*, 84(B7), 3519–3526.
- McClung, D. M., & Borstad, C. P. (2012). Deformation and energy of dry snow slabs prior to fracture propagation. *Journal of Glaciology*, 58(209), 553–564. <https://doi.org/10.3189/2012JoG11J009>
- McClung, D., & Schaerer, P. (2006). The Avalanche Handbook. *The Mountaineers Books*, 1–342.
- Moner, I., Gavaldà, J., Bacardit, M., Garcia, C., & Martí, G. (2008). Application of Field Stability Evaluation Methods to the Snow Conditions of the Eastern Pyrenees. *International Snow Science Proceedings, Whistler, British Columbia*, 386–392.
- Müller, K., Techel, F., Mitterer, C., Feistl, T., Sofia, S., Roux, N., Palmgren, P., Bellido, G. M., & Bertranda, L. (2023). The EAWS Matrix, A Look-Up Table for Regional Avalanche Danger Level Assessment, and its Underlying Concept. *International Snow Science Workshop, Bend, Oregon*, 540–546.
- Napadensky, H. (1964). Dynamic response of snow to high rates of loading. *US Army Material Command, Cold Regions Research & Engineering Laboratory*, 1–52.
- Norwegian Water Resources and Energy Directorate. (2022). *Felthåndbok for Snø og Skredobservasjoner* (J. Aasen, Ed.; 3rd Edition). Norwegian Water Resources and Energy Directorate.
- Perla, R. I., & LaChapelle, E. R. (1970). A theory of snow slab failure. *Journal of Geophysical Research*, 75(36), 7619–7627. <https://doi.org/10.1029/JC075i036p07619>
- Reuter, B., & Schweizer, J. (2018). Describing Snow Instability by Failure Initiation, Crack Propagation, and Slab Tensile Support. *Geophysical Research Letters*, 45(14), 7019–7027. <https://doi.org/10.1029/2018GL078069>
- Schweizer, J., & Jamieson, J. (2010). Snowpack tests for assessing snow-slope instability. *Annals of Glaciology*, 51(54), 187–194. <https://doi.org/10.3189/172756410791386652>
- Schweizer, J., Schneebeli, M., Fierz, C., & Föhn, P. M. B. (1995). Snow mechanics and avalanche formation: field experiments on the dynamic response of the snow cover. *Surveys in Geophysics*, 16(5–6), 621–633. <https://doi.org/10.1007/BF00665743>
- Shapiro, L., Johnson, J., Sturm, M., & Blaisdell, G. (1997). *Snow mechanics: review of the state of knowledge and applications*.
- Simenhois, R., & Birkeland, K. (2006). The Extended Column Test: A Field Test for Fracture Initiation and Propagation. *International Snow Science Workshop, Telluride, Colorado*, 79–85.



- Simenhois, R., & Birkeland, K. W. (2009). The Extended Column Test: Test effectiveness, spatial variability, and comparison with the Propagation Saw Test. *Cold Regions Science and Technology*, 59(2–3), 210–216. <https://doi.org/10.1016/j.coldregions.2009.04.001>
- Surowiecki, J. (2005). *The wisdom of crowds*. Anchor.
- 510 Techel, F., Winkler, K., Walcher, M., van Herwijnen, A., & Schweizer, J. (2020). On snow stability interpretation of extended column test results. *Natural Hazards and Earth System Sciences*, 20(7), 1941–1953. <https://doi.org/10.5194/nhess-20-1941-2020>
- Thumlert, S., & Jamieson, B. (2015). Stress measurements from common snow slope stability tests. *Cold Regions Science and Technology*, 110, 38–46. <https://doi.org/10.1016/j.coldregions.2014.11.005>
- 515 Toft, H. B., Verplanck, S. V., & Landrø, M. (2023). *Tap-o-meter data*. Open Science Framework. <https://doi.org/10.17605/OSF.IO/BV5PM>
- Tukey, J. (1977). *Exploratory data analysis* (Vol. 2).
- van Herwijnen, A., & Birkeland, K. W. (2014). Measurements of snow slab displacement in Extended Column Tests and comparison with Propagation Saw Tests. *Cold Regions Science and Technology*, 97, 97–103. <https://doi.org/10.1016/j.coldregions.2013.07.002>
- 520 van Herwijnen, A., Heck, M., & Schweizer, J. (2016). Forecasting snow avalanches using avalanche activity data obtained through seismic monitoring. *Cold Regions Science and Technology*, 132, 68–80. <https://doi.org/10.1016/j.coldregions.2016.09.014>
- Virtanen, P., Gommers, R., Oliphant, T. E., Haberland, M., Reddy, T., Cournapeau, D., Burovski, E., Peterson, P., Weckesser, W., Bright, J., van der Walt, S. J., Brett, M., Wilson, J., Millman, K. J., Mayorov, N., Nelson, A. R. J., Jones, E., Kern, R., Larson, E., ... Vázquez-Baeza, Y. (2020). SciPy 1.0: fundamental algorithms for scientific computing in Python. *Nature Methods*, 17(3), 261–272. <https://doi.org/10.1038/s41592-019-0686-2>
- Wakahama, G., & Sato, A. (1977). Propagation of a Plastic Wave in Snow. *Journal of Glaciology*, 19(81), 175–183. <https://doi.org/10.3189/S0022143000029269>
- 530 Weißgraeber, P., & Rosendahl, P. L. (2023). A closed-form model for layered snow slabs. *The Cryosphere*, 17(4), 1475–1496. <https://doi.org/10.5194/tc-17-1475-2023>
- Winkler, K., & Schweizer, J. (2009). Comparison of snow stability tests: Extended column test, rutschblock test and compression test. *Cold Regions Science and Technology*, 59(2–3), 217–226. <https://doi.org/10.1016/j.coldregions.2009.05.003>



Appendix



Appendix-1: The tap-o-meter was calibrated using known weights ranging from 5 to 30 kg.